Title

Competition between Dissolved Organic Matter and Freshwater Plankton Control Methylmercury Isotope Fractionation during Uptake and Photochemical Demethylation.

Journal

ACS Earth and Space Chemistry, 7(12)

ISSN

2472-3452

Authors

Armstrong, Grace

Janssen, Sarah

Tate, Michael

et al.

Publication Date

2023-12-21

DOI

10.1021/acsearthspacechem.3c00154

Peer reviewed

ACS EARTH AND SPACE CHEMISTRY

http://pubs.acs.org/journal/aesccq
Article

Competition between Dissolved Organic Matter and Freshwater Plankton Control Methylmercury Isotope Fractionation during Uptake and Photochemical Demethylation

Grace J. Armstrong, Sarah E. Janssen,* Brett A. Poulin, Michael T. Tate, David P. Krabbenhoft, and James P. Hurley

Cite This: ACS Earth Space Chem. 2023, 7, 2382−2392
Read Online

ACCESS | Metrics & More | Article Recommendations | Supporting Information

ABSTRACT: Isotope fractionation related to photochemical reactions and planktonic uptake at the base of the food web is a major uncertainty in the biological application of mercury (Hg) stable isotopes. In freshwater systems, it is unclear how competitive interactions among methylmercury (MeHg), dissolved organic matter (DOM), and phytoplankton govern the magnitude of mass-dependent and mass-independent fractionation. This study investigated how DOM alters rates of planktonic MeHg uptake and photodegradation and corresponding Hg isotope fractionation in the presence of freshwater phytoplankton species, *Raphidocelis subcapitata*. Outdoor sunlight exposure experiments utilizing *R. subcapitata* were performed in the presence of different DOM samples using environmentally relevant ratios of MeHg-DOM thiol groups. The extent of Δ^{199}Hg in phytoplankton incubations (2.99‰ St. Louis River HPOA, 1.88‰ Lake Erie HPOA) was lower compared to paired abiotic control experiments (4.29 and 2.86‰, respectively) after ∼30 h of irradiation, resulting from cell shading or other limiting factors reducing the extent of photodemethylation. Although the Δ^{199}Hg/Δ^{201}Hg ratio was uniform across experiments (∼1.4), Δ^{199}Hg/δ^{202}Hg slopes varied dramatically (from −0.96 to 15.4) across incubations with *R. subcapitata* and DOM. In addition, no evidence of Hg isotope fractionation was observed within *R. subcapitata* cells. This study provides a refined examination of Hg isotope fractionation markers for key processes occurring in the lower food web prior to bioaccumulation, critical for accurately accounting for the photochemical processing of Hg isotopes across a wide spectrum of freshwater systems.

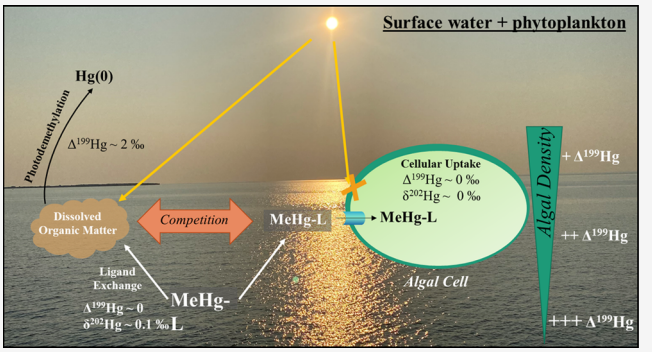

KEYWORDS: *mercury isotopes, photodegradation, uptake, phytoplankton, dissolved organic matter, freshwater*

INTRODUCTION

Mercury (Hg) is a ubiquitous contaminant recognized by the World Health Organization as a chemical of concern for public health due to its neurotoxic effects.[1,2] The highly bioaccumulative form of Hg, methylmercury (MeHg), is largely responsible for fish consumption advisories around the globe.[3] A major pathway in which MeHg enters aquatic food webs is through planktonic uptake and bioaccumulation, magnifying by a factor >10^4 from aqueous to phytoplanktonic concentrations.[4,5] Bioaccumulation of aqueous MeHg to phytoplankton is influenced by MeHg removal mechanisms, including photochemical degradation, a main mechanism of Hg loss in aquatic systems.[6−9] Within the water column of freshwater and marine aquatic environments, planktonic uptake of MeHg competes with photochemical degradation and other loss pathways of less significance, including biotic demethylation.[10] A better understanding of the competing factors governing the biologic uptake of MeHg and photodemethylation in plankton is vital for assessing bioaccumulation; yet, there are limited data about these processes in freshwater plankton species.

Planktonic uptake of MeHg and photochemical degradation are strongly influenced by the presence of dissolved organic matter (DOM), which forms strong complexes with MeHg through reduced sulfur groups[11−13] and acts as a photosensitized intermediate in the photodemethylation reaction.[9,14,15] Plankton also produce cell exudates, which are akin to DOM and mainly composed of biopolymers, refractory compounds similar to humic substances, and various neutral and low molecular weight acid compounds.[16] Mechanistically, phytoplanktonic MeHg uptake is largely known to be a passive

Received: June 5, 2023
Revised: November 20, 2023
Accepted: November 21, 2023
Published: December 6, 2023

Table 1. Sunlight Exposure Experimental Conditions for Plankton (*R. subcapitata*) Incubations across All Dissolved Organic Matter (DOM) Types[a]

	abbreviated condition	*n*	DOM type	[DOM] mg C L^{-1}	phytoplankton cell count (cells mL^{-1})
control	Dark ctrl, Biotic Williams L. HPOA[39]	1	Williams Lake, HPOA (2010)	11	400,000
	No DOM ctrl	2	Deficient Fraquil Media, cell exudates	<0.2	400,000
	Abiotic St. Louis R. HPOA	1	St. Louis River, mile 94 HPOA	18	none
	Abiotic L. Erie HPOA	1	Lake Erie − ER086 HPOA	19	none
experimental	Biotic St. Louis R. HPOA	2	St. Louis River, mile 94 HPOA	18	400,000
	Biotic Evergl. F1 HPOA[38,40]	3	Everglades F1 HPOA (2010)	3.75	400,000
	Biotic Williams L. HPOA[39]	2	Williams Lake, HPOA (2010)	11	400,000
	Biotic IHSS Suwannee R. FA[37,41]	1	IHSS Suwannee River Fulvic Acid Standard III, 3S101F	23	400,000
	Biotic L. Erie HPOA	3	Lake Erie − ER086 HPOA	19	400,000

[a]Abiotic controls did not contain phytoplankton cells, whereas the No DOM control contains phytoplankton cells and associated cell exudates. Incubations were performed at a uniform molar methylmercury (MeHg)/DOM thiol ratio of 0.01. Replicates for each condition are denoted in the *n* column.

process with the extent of uptake being a product of the phytoplankton cell surface area-to-volume ratio,[17] but there have also been indications of limited facilitated and active uptake.[5,18] Previous studies indicate that the competition between MeHg binding to DOM and planktonic uptake ultimately governs the bioaccumulation rate of MeHg in aquatic food webs.[19−23] Further, MeHg bound to DOM can limit the passive planktonic uptake of MeHg due to the large size and hydrophobicity of the DOM−MeHg complexes.[12,13,18−20]

Mercury stable isotopes are uniquely capable of tracking photochemical transformations due to the occurrence of both mass-dependent fractionation (MDF, denoted here by δ^{202}Hg) and mass-independent fractionation (MIF, denoted by Δ^{199}Hg and Δ^{201}Hg), most commonly induced via ultraviolet−visible (UV−vis) irradiation.[24−27] A study utilizing marine phytoplankton exposed to natural sunlight in the presence of MeHg in artificial seawater showed enhanced MIF during photodemethylation in the presence of cells and associated exudates in comparison to abiotic conditions absent of plankton, demonstrating that aquatic transformations of Hg prior to bioaccumulation are driven by photochemical and plankton-mediated processes that induce both MDF and MIF.[28] While the study was foundational in demonstrating that plankton influence the isotopic transformation of Hg, it remains the only information available on Hg isotope fractionation from photochemical reactions of MeHg with phytoplankton; it did not include effects of DOM type and was conducted under marine conditions.[28] Characterization of MeHg photodegradation in freshwater systems, distinguished by lower ionic strength and different complexation chemistries (including DOM), may confound the transferability of marine results. Further, the broad range of plankton species and DOM conditions[24,25,29] within natural environments may influence the magnitude of photochemical demethylation and subsequent Hg isotope fractionation. Researchers have shown that changes to the chemical speciation of MeHg can affect bacterial uptake and induce fractionation, resulting in another confounding factor when assessing MeHg uptake into phytoplankton.[30,31]

In this study, we investigated MeHg uptake and sunlight-induced isotopic fractionation in the presence of freshwater phytoplankton (*Raphidocelis subcapitata*) and natural DOM samples to fill essential knowledge gaps regarding Hg isotope transformations at the base of the freshwater food web. We hypothesized that MeHg uptake and photochemical demethylation would be controlled by competitive interactions of MeHg with DOM and phytoplankton, and that photoinduced Hg isotope fractionation patterns observed previously in marine phytoplankton would be mirrored in freshwater species (*R. subcapitata*). We tested these hypotheses through a series of uptake and sunlight exposure experiments with commercially available (Suwannee River fulvic acid) and natural DOM samples from critical freshwater ecosystems including the Florida Everglades and Laurentian Great Lakes. The findings presented here are the first comprehensive examination of Hg isotope fractionation during uptake and photochemical demethylation of MeHg in the presence freshwater phytoplankton cells, which is vital to confidently apportion environmental sources of Hg to biological Hg burdens.

METHODS

Phytoplanktonic Cultures. All phytoplankton incubation experiments were conducted utilizing *R. subcapitata*, formerly known as *Selenastrum capricornutum* (UTEX 1648), a freshwater unicellular green phytoplankton species that has been used as a test organism in previous MeHg uptake studies[18,19] and as a U.S. Environmental Protection Agency test organism (EPA Method 1003.0).[32] *R. subcapitata* was utilized in this study because it is naturally present in freshwater ecosystems and is easy to culture in a laboratory setting. Cultures were maintained in an environmental chamber at 20 °C under continuous white fluorescent lighting (∼940 Lux) and were aerated utilizing a vacuum pump equipped with a 0.22 μm particulate filter. Batch phytoplankton cultures were grown in autoclave-sterilized Bold's Basal Medium (BBM),[33,34] in acid-washed 250 mL Erlenmeyer flasks (preinoculum) covered with a beaker and 6 L flat-bottom boiling flasks (batch culture) topped with a double-holed silicone aeration stopper. *R. subcapitata* preinoculum (200 mL) was grown for 7 days and transferred into 6 L flasks (4 L of BBM) using sterile procedures and grown for another 7 days followed by 4 days of settling. Once settled, 3 L of media was poured off, and cultures were counted using a flow cytometer. Cultures were checked for contamination routinely using Luria−Bertani broth[35] and a light microscope. Modified Fraquil Media (FM),[36,37] deficient in copper, zinc, and ethylenediaminetetraacetic acid (EDTA), was utilized during experiments to

https://doi.org/10.1021/acsearthspacechem.3c00154
ACS Earth Space Chem. 2023, 7, 2382−2392

minimize competitive interactions between copper and zinc during phytoplankton uptake and to avoid complexation of MeHg by EDTA. Fraquil was filter-sterilized using a 0.22 μm capsule filter and a peristaltic pump. Media was adjusted to approximately pH 7 to match phytoplankton culture media. For all MeHg uptake and sunlight exposure experiments, cultures were diluted with sterile media and transferred into 1 L of acid-cleaned quartz reactors prior to MeHg and DOM exposure to prevent wall loss.

Dissolved Organic Matter Collection and Characterization. Five DOM samples were used in this study (Table 1), either purchased from the International Humic Substances Society (IHSS)[38] (Suwannee River Fulvic Acid, SRFA), or isolated by the U.S. Geological Survey (USGS) Organic Geochemistry Laboratory in Boulder, Colorado (SI Section S1, Tables S1−S3, and Figure S1).[39] Aqueous hydrophobic organic acid (HPOA) was isolated from four contrasting environments including marshlands (Florida Everglades site F1),[39] a seepage lake (Williams Lake, Minnesota),[40] a eutrophic Great Lake (Lake Erie), and a Great Lakes tributary (St. Louis River, Minnesota) (Table S1). These sites were chosen to represent the heterogeneous composition of the DOM corresponding to a range of freshwater aquatic ecosystems. Details regarding the isolation and characterization of DOM samples are provided in the Supporting Information Sections S1−S3. Briefly, DOM samples were characterized for ultraviolet and visible light (UV−vis) optical parameters, including specific UV absorbance at 254 nm ($SUVA_{254}$) and light attenuation at 254 nm (Table S1). Further, the organic sulfur content and organic sulfur speciation of DOM samples were characterized previously for two of the DOM samples (IHSS SRFA, Everglades F1 samples),[41,42] and were measured for elemental composition and sulfur K-edge X-ray absorption near edge structure (XANES) spectroscopy on the other 3 DOM samples for this study (Tables S2−S3 and Figure S1). For experiments, solid DOM samples were reconstituted in buffered aqueous solutions (pH 7) in autoclaved volumetric flasks using sterilized modified FM (Table 1). Importantly, pH of 7 was selected for these experiments to match and maintain *R. subcapitata* cultures, and it has been demonstrated that Hg and MeHg binding strength to DOM is conserved across a wide pH range.[13,43]

Phytoplankton MeHg Uptake Experiments. Uptake experiments examined the extent of isotope fractionation during MeHg uptake by *R. subcapitata*. Experimental conditions included a no DOM condition absent of any added DOM but containing cell exudates (n = 1), a low DOM concentration SRFA condition (1 mg L^{-1}, n = 2), and a high DOM concentration SRFA condition (23 mg L^{-1}, n = 2). Each condition was assessed in foil-covered reactors to simulate dark conditions. Cultures of *R. subcapitata* (400,000 cells mL^{-1}) were equilibrated with fresh sterile media and DOM for 1−2 h prior to experiments. Reactors were then spiked with approximately 3.5 ng mL^{-1} MeHg and the first time point sample was immediately collected. We selected this MeHg spike concentration because it was an order of magnitude lower than previous photochemical Hg isotope studies[24,25] yet still allowed for the measurement of Hg isotopes in the dissolved phase. Samples were collected over the course of 48 h to capture the uptake of MeHg into *R. subcapitata*. Four different Hg samples were collected at each time point including total Hg (cellular bound and dissolved phase), dissolved phase Hg, cell-associated (extra and intracellular) Hg, and intracellular Hg. Complete details on the collection and wash protocols[21] are provided in the Supporting Information Section S4. All samples were preserved to a final volume of 10% acid content with equal volumes of nitric acid (5% HNO_3, EMD Millipore) and bromine monochloride (BrCl) to ensure full oxidation of MeHg in the sample to inorganic Hg(II). Additional acid rinses were obtained from each reactor to assess the potential sorption of MeHg to the quartz reactor walls. After the last time point (t = 72 h), each reactor was emptied and rinsed with deficient fraquil to remove all spiked experimental media. Once the reactors were empty, they were rinsed with 10% HCl and analyzed for HgT (Table S7). Loss of MeHg to wall sorption was minimal, averaging 0.10 ± 0.08 ng mL^{-1}, or <3% of starting MeHg content.

Sunlight Exposure Experiment. Photodegradation of MeHg was examined in an outdoor sunlight exposure study. The experiment included phytoplankton (*R. subcapitata*) incubations, four DOM samples isolated for this work, and a 23 mg L^{-1} SRFA (IHSS) DOM sample for comparison with the uptake experiments outlined above (Table 1). Previous research concluded that the DOM thiol content was an important factor influencing the degree of MIF during MeHg demethylation across DOM types.[25] Therefore, in this study, all sunlight exposure conditions were performed at a uniform molar ratio of MeHg/DOM thiol of 0.01 (i.e., 100-fold higher DOM thiol concentration than MeHg in solution). This ensured that there was an overabundance of strong binding DOM thiol sites to complex MeHg. Thus, experimental vessels with different DOM types had variable DOM concentrations (3.75−23 mg L^{-1}, Table 1). The outdoor sunlight exposure experiment was conducted over 3 days in ambient sunlight at the USGS Mercury Research Laboratory (MRL, Madison, WI). The experiment was performed on sunny days with minimal cloud coverage and solar intensity was monitored using an Apogee Pyranometer SP-215 (intensity profiles are shown in Figure S2).[44]

Experimental treatments were: (1) A dark control treatment assessed MeHg loss in the absence of sunlight; (2) Two phytoplankton-free (abiotic) treatments investigated abiotic sunlight treatments paired to phytoplankton incubations; (3) A no DOM control treatment (absent of added DOM but containing cell exudates) was used to understand how the presence of phytoplankton cells and their associated exudates affect MeHg photodegradation; and (4) A cell count flask (no MeHg amendment) was included to quantify any phytoplankton cell density fluctuations due to cell settling or growth. From tested aliquots, cell counts fluctuated minimally from 512,820 cells mL^{-1} (0 h) to 829,190 cells mL^{-1} (~50 h) (Table S4). Information about experimental replicates (n) can be found in Table 1.

Prior to sunlight exposure, reactors were covered with foil and pre-equilibrated for 24 h with modified media (FM, FM + DOM) inoculated with *R. subcapitata* culture (400,000 cells mL^{-1}) and a 2 ng mL^{-1} MeHg chloride (MeHgCl, Brooks Rand) spike; pre-equilibration conditions were based on MeHg uptake experiments and previous assessments.[28] Media blanks for each condition (<0.04 ng L^{-1}, containing FM, DOM, and cells), taken before adding the MeHg spike, were analyzed for total mercury (HgT) prior to experiments.[28] After equilibration, reactors were placed outside in a 20 °C water bath to prevent phytoplankton heat stress and were exposed to sunlight for 50 h. It is important to note that all of the reactors were treated similarly in the circulating bath (e.g.,

https://doi.org/10.1021/acsearthspacechem.3c00154
ACS Earth Space Chem. 2023, 7, 2382−2392

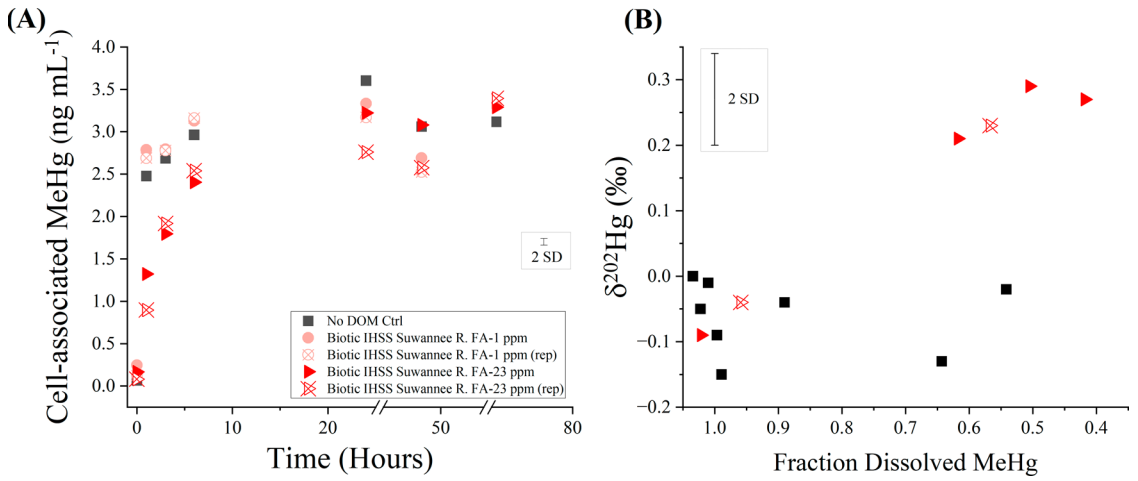

Figure 1. (A) Uptake of cell-associated MeHg in *R. subcapitata* under different DOM conditions and (B) δ^{202}Hg values in the dissolved phase during Hg uptake. Error bars represent the 2SD of (A) the Hg concentration detection limit and (B) δ^{202}Hg measured in a NIST RM 8610 instrument (n = 110).

equally submerged and spaced); however, the use of the bath itself could dampen the full extent of sun exposure, albeit uniformly across conditions. All reactors were continuously purged using ambient air (pre-scrubbed with in-line gold traps to prevent Hg contamination). At predefined time points, samples of total Hg and dissolved phase Hg were collected using the methods outlined above for uptake experiments. Intracellular and cell-associated Hg fractions were not directly collected due to logistical concerns, specifically the transport of samples from outdoor reactors to the manifold filtration apparatus; thus, the cell-associated Hg fraction was calculated by the difference between the total mercury and dissolved phase for photochemistry experiments. Additional samples for dissolved organic carbon (DOC) analysis were collected into 40 mL amber glass vials prior to and at the end of sunlight exposure to determine the extent of photochemical mineralization of DOM. DOC samples were analyzed on a total organic carbon analyzer (Shimadzu TOC-L, limit of detection 0.4 μg L^{-1}) using standard methods.[45] Photomineralization of DOM during light exposure was expected to be minimal based on experiments conducted in similar reaction vessels and a photosimulator.[46] Yet, an average of 75% of the DOC was recovered at the end of experiments over the 50 h of sunlight irradiance, interpreted to reflect minor contributions of photomineralization of DOM and other more prominent removal processes (i.e., absorption of DOM to *R. subcapitata*, microbial degradation[47]) (Table S5).

Hg Concentration and Isotope Analysis. MeHg from both uptake and sunlight exposure experiments was measured as HgT (EPA Method 1631 at the USGS MRL). Inorganic Hg was not expected to be present in aqueous solution, since no reductive loss was observed in the uptake experiment, and the sunlight exposure experiment employed continuous purging to ensure the removal of any reduced Hg(0) product. Briefly, oxidized samples were neutralized using hydroxylamine hydrochloride and reduced with tin chloride ($SnCl_2$) to convert aqueous Hg(II) to gaseous Hg(0). Gaseous Hg was purged onto gold traps and analyzed via cold vapor atomic fluorescence spectrometry (CVAFS, limit of detection 0.20 ng L^{-1}). After HgT analysis, samples were measured for the Hg stable isotope composition. Dissolved Hg aliquots with concentrations less than 1 ng mL^{-1} were preconcentrated using a rapid thermal desorption and chemical oxidant method prior to isotope analysis.[48] Preconcentration involved the chemical reduction and preconcentration of Hg onto gold traps, followed by thermal desorption of Hg into an oxidizing chemical trap solution (40% $3HNO_3$/1BrCl).[48]

Samples were analyzed for Hg stable isotope ratios using a multicollector inductively coupled mass spectrometer (MC-ICP-MS, Neptune Plus, Thermo Scientific). Mercury samples were introduced into the MC-ICP-MS using a gas−liquid separator, and an internal thallium standard was simultaneously introduced using a desolvating nebulizer for mass bias correction.[49] Aliquots of samples were diluted to a Hg concentration of 0.5 to 1 ng mL^{-1} and a final acid concentration less than 10%. Samples were analyzed using standard sample bracketing with National Institute of Standards and Technology (NIST) 3133. Bracketing standard and secondary standard UM Almaden (NIST RM 8610) were diluted to match the acid matrix and Hg concentration of the samples. Instrumental parameters (i.e., lenses, gas levels, and peak shape) were tuned daily using NIST 3133 and optimized for intensity and stability of Hg signal (approximately 1 V per 1 ng mL^{-1} Hg).[48,49] The instrument monitored 8 total Faraday cups for ^{203}Tl and ^{205}Tl and for six Hg isotopes (^{198}Hg, ^{199}Hg, ^{200}Hg, ^{201}Hg, ^{202}Hg, ^{204}Hg). Delta values were calculated using established methods (SI Methods).[50] Accuracy and precision of isotope measurements was quantified using NIST RM 8610 analyzed alongside experimental samples (δ^{202}Hg = −0.55 ± 0.07‰, Δ^{199}Hg = −0.03 ± 0.06‰, Δ^{200}Hg = 0.01 ± 0.05‰, Δ^{201}Hg = −0.04 ± 0.06‰, and Δ^{204}Hg = −0.00 ± 0.10‰; 2 standard deviation (SD), n = 110), which agreed with reported values.[51] All Hg concentration and Hg stable isotope data is available in the corresponding data release.[44]

RESULTS AND DISCUSSION

Isotopic Fractionation during Phytoplanktonic Cellular Uptake of MeHg. Cellular uptake of MeHg in the dark was investigated under both no DOM (containing only cells and cellular exudates), low DOM (1 mg L^{-1} SRFA), and high DOM (23 mg L^{-1} SRFA) conditions for *R. subcapitata*. Under conditions of no DOM and low DOM-SRFA, MeHg uptake by *R. subcapitata* occurred rapidly in the first hour of exposure resulting in an average increase of 2.41 and 2.55 ng mL^{-1} in

https://doi.org/10.1021/acsearthspacechem.3c00154
ACS Earth Space Chem. 2023, 7, 2382−2392

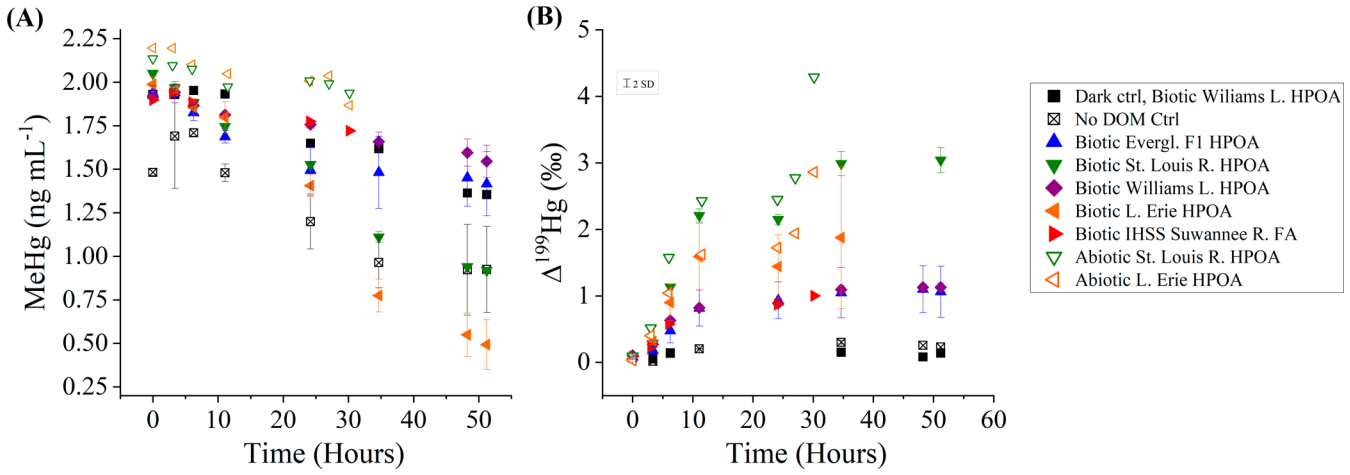

Figure 2. Sunlight exposure experiment (MeHg + DOM + phytoplankton) trends for (A) MeHg loss and (B) Δ^{199}Hg values of residual MeHg. Closed symbols represent biotic conditions (with *R. subcapitata*), whereas open symbols represent abiotic conditions. Error bars on individual points indicate 1 SD of the experimental replicates. The 2 SD box represents precision of Δ^{199}Hg measurements as quantified using the NIST RM 8610 standard (n = 110).

cell-associated filter digests, respectively (Figure 1A). After one h of exposure, the majority of MeHg was cell-associated in the no DOM condition (62%, of which 53% was intracellular) and under the low DOM-SRFA condition (71%, with 48% intracellular). After 24 h, MeHg uptake to *R. subcapitata* plateaued for the remainder of the 72 h exposure (Figure 1A). Importantly, under the high DOM-SRFA conditions, the cell-associated MeHg pool showed a slower uptake. The cell-associated MeHg pool increased by only 0.98 ng mL^{-1} after the first hour of exposure, equating to 29% of MeHg being cell-associated. MeHg uptake under the high DOM-SRFA condition continued slowly until 24 h into the exposure. All treatments demonstrated equivalent decreases in the dissolved phases resulting in <20% MeHg remaining in the dissolved phase after 72 h of exposure. All MeHg added to incubation flasks was accounted for in the no DOM (93.72 ± 4.88%), low DOM-SRFA (97.97 ± 6.98%), and high DOM-SRFA (97.55 ± 5.63%) conditions across all time points.

In addition, no measurable Hg(0) loss was observed from cultures, which is consistent with the expectation that biologic reduction would only occur in the presence of inorganic Hg.[30,52] These observations align with previous surveys of phytoplankton and provide additional evidence that competition between DOM and plankton cells will alter MeHg uptake rates.[19−22] We do note that the MeHg concentrations used in these experiments exceed natural concentrations and that cellular uptake at lower MeHg concentrations may be substantially less, similar to patterns demonstrated in field comparisons of oligotrophic and eutrophic systems.[53]

Hg isotopes were measured in the dissolved phase of uptake incubations for no DOM and high DOM conditions to assess the extent of isotope fractionation. Under the no DOM condition, δ^{202}Hg of the dissolved MeHg fluctuated between −0.01 to −0.13‰ over the course of the MeHg uptake exposure (Figure 1B). After the first half hour, δ^{202}Hg increased from −0.08 to −0.01‰ in the dissolved phase and stayed constant through the remainder of the exposure. The observed modest increase in δ^{202}Hg is similar to observations made in wild type and mutant bacterial strains of *Geobacter sulfurreducens* exposed to MeHg, though these levels did not exceed analytical uncertainty of Hg isotope measurements.[30]

The δ^{202}Hg values of the cell-associated phase, which were limited by Hg mass and could only be measured at later time points when more Hg was associated with the cell (Figure 1A), ranged from −0.16 to −0.11‰ at 24 and 48 h, respectively. However, δ^{202}Hg values for both dissolved and cell-associated MeHg were within the analytical error of Hg isotope measurements, indicating that Hg isotope fractionation due to MeHg uptake was negligible under no DOM or low DOM conditions.

The δ^{202}Hg values of dissolved MeHg under the high DOM-SRFA condition showed a modest increase from −0.07 to 0.22‰ in the first hour and then stabilized to 0.29 and 0.27‰ after 3 and 6 h, respectively. MeHg concentrations in the dissolved phase were too low for isotope measurements after the 6 h time point, but cell-associated δ^{202}Hg (0.11‰) was measured at the end of the exposure. We note that the cell-associated δ^{202}Hg under higher DOM-SRFA conditions is positive in comparison to the low DOM-SRFA conditions and deviates from the starting isotopic composition of the spike. Unlike the no DOM condition, δ^{202}Hg shifts were greater under the high DOM-SRFA conditions and above the analytical detection limit. These results indicate that minor MeHg mass-dependent fractionation occurs during the observed time window and is more pronounced under higher DOM conditions. Dissimilar to bacterial cultures,[30] we do not attribute isotope changes to active uptake due to the lack of fractionation under the no DOM conditions. Instead, we hypothesize that MeHg aqueous species equilibration between MeHgCl and organic carbon[13] results in a consistent isotopic shift (approximately 0.2‰) prior to cellular uptake. This would also account for the larger δ^{202}Hg value observed in the cell-associated measurement. Our observations are supported by a previous study examining inorganic Hg sorption to geothite, which reported an enrichment factor of a similar magnitude (0.3−0.4‰) for chemical species equilibration.[54] In summary, the results from these experiments demonstrate that uptake induces little to no fractionation in *R. subcapitata* during passive uptake but suggests that equilibration fractionation between MeHg and DOM species can alter the δ^{202}Hg value prior to or during cell association.

https://doi.org/10.1021/acsearthspacechem.3c00154
ACS Earth Space Chem. 2023, 7, 2382−2392

Influence of DOM and Phytoplankton Cells on MeHg Photodemethylation. To examine the extent of photodegradation in the presence of *R. subcapitata* and natural DOM isolates, we exposed *R. subcapitata* cultures to ambient sunlight to mimic environmental conditions. MeHg loss was observed across all light-exposed flasks, including abiotic (no cells), no DOM (cells and cellular exudates only), and natural DOM conditions (Figure 2A). We hypothesize that the majority of the observed decline in MeHg concentrations with irradiance time is largely attributable to photodegradation of MeHg,[6,9] which aligns with the expected mechanism in which the MeHg is photochemically degraded to gaseous elemental Hg(0), and was purged from the reactor. The rates of MeHg loss in DOM and phytoplankton experiments varied across natural DOM isolates (slowest rate, IHSS Suwannee River FA ≈ Williams L. HPOA < Everglades F1 HPOA < St. Louis R. HPOA < L. Erie HPOA, fastest rate; Table S6), and the relationship between natural DOM and MeHg loss was complex in the presence of phytoplankton (Figure 2). Specifically, each DOM condition, in association with *R. subcapitata*, appeared to have a unique effect on the extent or rate of MeHg loss. It is important to note that there were unexpected, slightly lower MeHg concentrations in the reactors at the first sample collection (t = 0 h, Figure 2A), possibly due to equilibration factors that were not accounted for in the original experimental design, including temperature change (e.g., moving from refrigeration to outside ambient temperature), sample transport, and preparation for outdoor experimental conditions (e.g., connecting purge lines, equilibrating water bath). Hence, we utilized t = 3 h to assess MeHg loss percentage and rates more accurately across all conditions. Over the course of sunlight exposure experiment with phytoplankton and DOM (~50 h), we observed the smallest decrease in MeHg concentration in the presence of Williams L. HPOA (loss of 0.40 ± 0.15 ng mL^{-1}) and the largest decrease in MeHg concentration in the presence of L. Erie HPOA (loss of 1.46 ± 0.16 ng mL^{-1}) (Figure 2A).

We also noted a decrease in the MeHg concentration for the dark control (loss of 0.58 ng mL^{-1}), which also contained *R. subcapitata*. Loss in the dark control exceeded the presumed photochemical losses in the biotic conditions for Williams L. HPOA and IHSS Suwannee R. FA (Figure 2A). At earlier time points, the dark control also exceeded the abiotic conditions, but we could not directly make the comparison out to the 50 h time point. Because there was no sunlight exposure for this flask, we attribute this decline to biologically mediated demethylation.[55,56] We saw no evidence of MeHg demethylation in uptake experiments with *R. subcapitata*, but it is possible that the longer exposure time (24 h pre-equilibration plus photochemical experiment duration) stressed the cells and resulted in MeHg loss, though only inorganic Hg loss has been recorded in past investigations of phytoplankton.[56,57] It is more likely that given the experimental conditions (outdoor, nonsterile sampling) the cultures were not completely axenic over the light exposure period, potentially giving rise to additional microbial growth capable of MeHg demethylation and reduction (e.g., *merA* or *merB*)[58] leading to isotope fractionation,[59] though this was not evaluated directly through microbial assays. To assess this anomaly in the dark control, we also completed a 30 h follow-up dark experiment including 1 abiotic control and 3 biotic replicates, each containing 1 mg L^{-1} IHSS Suwannee R. FA following similar methodology as the original photochemistry experiment. In this additional experiment, we observed no loss in HgT (Table S8), likely because the new cultures being used did not have microbial contamination. These results, combined with those outlined above, lead us to attribute MeHg loss in the reactors to a mixture of photochemical demethylation and microbial "dark" demethylation, which mirrors natural conditions in which both processes would be co-occurring. It is also important to note that with the observed loss in the dark control, we must also surmise that the losses in the sunlight-exposed reactors represent a mixture of microbial and photochemical degradation. Hence, to further decipher the extent of photochemical demethylation occurring across sunlight-exposed flasks, we examined the temporal variation in Δ^{199}Hg, a known tracer of photochemical degradation in natural systems.[60,61]

The residual MeHg in the reactors demonstrated increasing Δ^{199}Hg values over the course of the sunlight exposure. The increase in Δ^{199}Hg was greatest in St. Louis R. HPOA condition (Δ^{199}Hg increased 2.96 ± 0.20‰ from t = 0 to 51.2 h) and least in the Everglades F1 HPOA condition (Δ^{199}Hg increased 0.98 ± 0.42‰ from t = 0 to 51.2 h) (Figure 2B). The average variability in Δ^{199}Hg of the residual MeHg in the presence of phytoplankton and natural DOM conditions was 0.31‰ for triplicates (minimum of ±0.02‰, maximum of ±1.07‰) and 0.06‰ for duplicates (minimum of ±0.00‰, maximum of ±0.19‰), respectively. The photochemical slopes (Δ^{199}Hg/Δ^{201}Hg) of the biotic DOM conditions were similar (1.28−1.46, Table S6) to conditions without phytoplankton (1.4), all of which fall within the previously established range for photochemical demethylation (~1.2−1.41).[24−26,62] We observed no evidence of photoreduction of Hg(II), which is characterized by a Δ^{199}Hg/Δ^{201}Hg slope closer to 1.0,[24] though we cannot completely rule out the occurrence of dark oxidation of Hg(0) back to inorganic Hg within the reactors.[63] The dark control exhibited no discernible difference in Δ^{199}Hg values (0.07‰), supporting that the measured MeHg loss in the reactor was not photochemically mediated.[64]

We hypothesize that Hg-ligand interactions driven by the amount and type of DOM present in the reactor influenced photodegradation and resulted in different extents of MIF across DOM isolates, as observed in other studies[62,65] for inorganic Hg. However, we observed no discernible trends with MeHg loss or Δ^{199}Hg when compared to DOM characteristics (Tables S1 and S2), which makes it difficult to decipher specific factors driving enhanced MIF. We surmise that the lack of pattern between isotope values and DOM characteristics in the biotic reactors is due to the presence of cellular exudates, which have some similar components as DOM[16] and would be uncharacterized contributors to photochemical degradation of MeHg.

When comparing abiotic reactors to biotic reactors, lower Δ^{199}Hg values were observed in experiments with *R. subcapitata* (Figure 2B). For the St. Louis R. HPOA conditions, the residual MeHg in biotic reactors were on average 1.30 ± 0.18‰ lower in Δ^{199}Hg after 30 h of irradiance compared to abiotic reactors, whereas L. Erie HPOA conditions were 0.99 ± 1.07‰ lower in biotic versus abiotic reactors (Figure 2B). These results demonstrate the possibility that plankton cells may inhibit photodemethylation and subsequent MIF. The Δ^{199}Hg results, in addition to MeHg uptake experiments, indicate that once MeHg is taken up by phytoplankton it is "protected" from DOM-mediated photodegradation. Overall, we propose three mechanisms that could

https://doi.org/10.1021/acsearthspacechem.3c00154
ACS Earth Space Chem. 2023, 7, 2382−2392

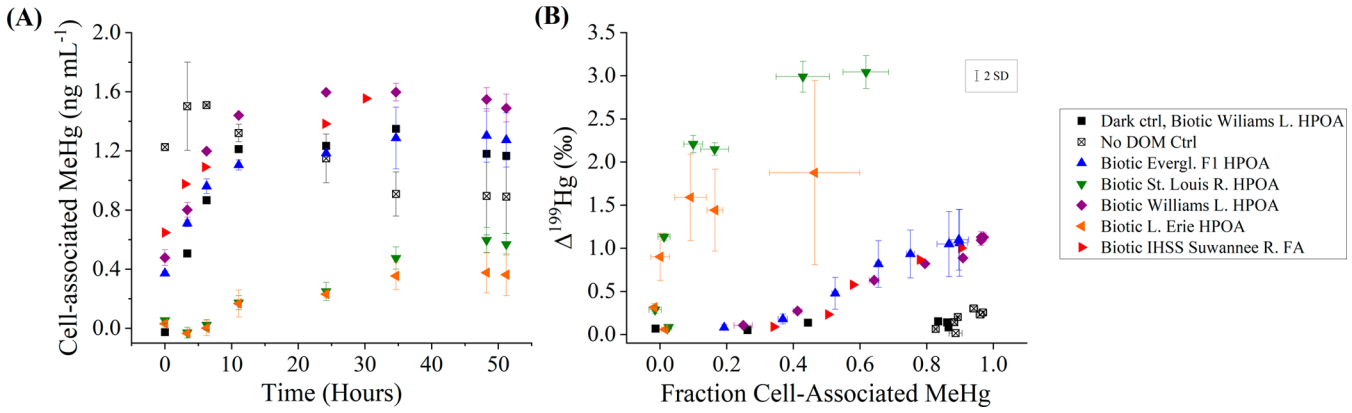

Figure 3. Sunlight exposure experiment, phytoplankton-mediated trends including (A) cell-associated MeHg concentrations over time and (B) Δ^{199}Hg versus the fraction of cell-associated MeHg. Closed symbols represent biotic conditions (with *R. subcapitata*). 2 SD represents the precision of Δ^{199}Hg measurements as quantified using the NIST RM 8610 standard (n = 110).

result in lower MIF in the presence of cells: (1) cellular shading in the reactor flasks, (2) cellular uptake of MeHg, and (3) loss of MeHg via microbial degradation prior to photodegradation. In the case of cellular shading, phytoplankton cells could shade aqueous MeHg from sunlight exposure, leading to reduced exposure to UV−vis irradiation and therefore, lower MIF extent. Similarly, the process of senescence (e.g., an increase in aging or dead plankton cells) could filter or limit the extent of UV−vis irradiation that reaches the MeHg and consequentially reduce photodegradation. The formation of cell exudates could also dampen photochemistry by scavenging free radicals,[66] effectively reducing photodegradation rates.[67] These results are contrary to previous findings by Kritee et al. which observed enhanced MIF in the presence of a marine species of phytoplankton and associated exudates.[28]

Cellular uptake of MeHg was also shown to be an important factor controlling Δ^{199}Hg patterns for sunlight exposure experiments with phytoplankton and DOM. The importance of the kinetics of cellular MeHg uptake and Hg isotope fractionation from sunlight is demonstrated in Figure 3, which presents cell-associated MeHg concentrations over time and their associated isotopic fractionation. In MeHg uptake experiments with high DOM concentration, we observed that MeHg uptake reaches a plateau after a rapid onset (Figure 1B), which is over the time periods of the sunlight exposure experiments (Figure 3A). For example, the St. Louis R. HPOA and L. Erie HPOA conditions exhibited the slowest uptake as evidenced by the smallest increases in the fraction of cell-associated MeHg (0.62 ± 0.07 and 0.72 ± 0.08, respectively) and highest extents of Δ^{199}Hg (Figure 3B). These observations indicate that passive uptake of MeHg was still occurring under the DOM conditions when the reactors were exposed to ambient sunlight, despite the 24 h pre-equilibration period. Thus, higher concentrations of DOM result in slower phytoplanktonic uptake of MeHg when compared to the lower concentration and biotic control reactors. This was also evidenced in the DOM conditions, especially in the St. Louis R. HPOA and L. Erie HPOA which exhibited the slowest uptake (Figure 3A) and highest Δ^{199}Hg over 50 h (Figures 2B and 3B). Although there is evidence of a concentration dependence for uptake as mentioned above, there are other factors related to DOM type that can alter uptake rates such as size, hydrophobicity, and associated ligands,[12,18−20,23] which were outside of the scope of this project due to the complexity that cellular exudates add to OM composition.

In contrast to Δ^{199}Hg patterns, δ^{202}Hg values during this experiment resulted in no discernible pattern under conditions with phytoplankton, often within the uncertainty of δ^{202}Hg measurements (Figure S3). The variable δ^{202}Hg values are likely the result of numerous simultaneous processes occurring in the reactors that can fractionate isotopes, including chemical species equilibration (discussed above),[54] potential biologically mediated reduction (observed in dark control), and MeHg photodegradation.[68]

Environmental Application of Hg Stable Isotopes. The interface of photochemistry and planktonic uptake is important for the application of Hg stable isotopes in tracing Hg sources to biological matrices. Previous work demonstrated that MIF is dependent on the DOM amount and chemical composition,[24,25,65] but our work adds an additional level of complexity by demonstrating that cellular processes (e.g., uptake, microbial demethylation) and cell-DOM interactions can greatly dictate the amount of MIF observed in the environment. Our work also shows that planktonic uptake of MeHg does not induce major Hg isotope fractionation of δ^{202}Hg, counter to previous bacterial studies,[30] but that equilibrium fractionation at high DOM concentrations can alter measured cell-associated values. In the environment, we anticipate that low DOM systems will support higher photochemical fractionation due to light penetration as supported by previous work.[69,70] However, our biotic results indicate phytoplanktonic uptake of MeHg, which would also be favored under lower DOM conditions and DOM of lower aromatic composition,[22] results in lower Δ^{199}Hg values due to shielding within the cells. When examining MeHg photodemethylation in the environment, both chemical and biological factors differ between aquatic environments, which may result in the variability in Δ^{199}Hg observed in fish from lakes,[69] streams,[71] and ocean basins.[70,72−74] Factors including light penetration depth (water clarity) and plankton density are expected to play key roles in Hg isotope fractionation and further examination of phytoplankton and waters would be needed to fully examine the mechanistic interplays of phytoplankton cells and photochemical reactions in natural waters.[75]

Applying our results to environmental systems, the photochemical slopes (Δ^{199}Hg/ Δ^{201}Hg) presented in the sunlight

https://doi.org/10.1021/acsearthspacechem.3c00154
ACS Earth Space Chem. 2023, 7, 2382−2392

exposure experiment aligned with values observed in environmental fish tissue samples from the St. Louis R. (*Micropterus dolomieu*-Smallmouth Bass, *Catostomus commersonii*-White Sucker, *Esox lucius*-Northern Pike) and Florida Everglades (*Hemichromis letourneuxi*-African Jewelfish, *Gambusia affinis*-Western Mosquitofish),[44] which are near the locations where two of the DOM samples were collected (Figure S4). This observation supports that the experimental measurements of $\Delta^{199}Hg/\Delta^{201}Hg$ slopes (Figure S4) reflect photochemical signatures observed in actual biota samples,[24] suggesting that MIF during photochemical demethylation is a generally conserved signature under environmentally relevant MeHg-DOM ratios and in the presence of plankton cells, but the extent of the reaction is dictated by other factors in the water column (e.g., DOM type and concentration, presence of algal cells).

Our observations also have important implications for how Hg isotope sources relate to MeHg bioaccumulation. Often, Hg sources in the environment (e.g., sediments, terrestrial reservoirs, precipitation) are disconnected from Hg isotope values measured in biological tissue, likely due in part to the imprint of photochemical demethylation in the water column. Due to the observed consistency of MIF during photochemical demethylation across ecosystems, as determined from $\Delta^{199}Hg/\Delta^{201}Hg$ slopes,[61] $\Delta^{199}Hg$ and $\delta^{202}Hg$ relationships have been used to correct for photochemical processes and estimate the source of MeHg to biota.[70,76,77] It is common for the slope of $\Delta^{199}Hg/\delta^{202}Hg$ to be used to correct $\delta^{202}Hg$ for photochemical demethylation, using a slope of 2.43 for waters with 1 mg L^{-1} DOM and 4.79 for waters with 10 mg L^{-1} DOM.[24] However, in this study, $\Delta^{199}Hg/\delta^{202}Hg$ slopes spanned a large range of values (−0.96 to 15.41) based on different natural DOM types and concentrations (Table S6), which has also been observed but not addressed in other studies.[24−26] We also observe large error within these slopes (Table S6) for algal incubations, which we attribute to additional processes such as cellular uptake and dark biotic reduction of MeHg, which alter the $\delta^{202}Hg$ value but not the $\Delta^{199}Hg$ extent. Furthermore, the large range of slopes across DOM isolates mirrors those observed in Chandan et al. (0.50 to 12.84)[25] demonstrating that the natural range of $\Delta^{199}Hg/\delta^{202}Hg$ well exceeds the benchmarks set forth for photochemical corrections. The large error in $\Delta^{199}Hg/\delta^{202}Hg$ slopes within this study coupled to the range of slopes observed here and in other studies highlights the difficulty in directly applying these metrics for photochemical correction across diverse ecosystem types.[70,77]

The large range of $\Delta^{199}Hg/\delta^{202}Hg$ slopes could result in vastly different corrected values of $\delta^{202}Hg$ for MeHg sources and food webs. While correcting $\delta^{202}Hg$ values for photochemical processes has been useful in assessing marine sources of MeHg, comparing different regional sources,[66,69] and for normalization of isotope values between fish species,[61] the variation in $\Delta^{199}Hg/\delta^{202}Hg$ observed in this study raises concerns for universal application of a single correction across freshwater ecosystems. We especially call for caution in applying these corrections across diverse ecosystem settings (e.g., lakes, rivers, and wetlands) with different water characteristics, particularly DOM, a focus of this study. Our work further highlights that photochemical corrections can misrepresent sources of MeHg to the food web and demonstrates the need to integrate direct measurements of MeHg isotopes[78−80] or other mathematical isotope estimates[81,82] to connect MeHg produced in the environment to biological burdens. The stark discrepancy in the MDF and MIF observed in our freshwater phytoplankton-mediated photochemistry experiments versus previous work incorporating marine phytoplankton[28] suggests that the role plankton plays in photochemical transformations is still unknown and varies across plankton species and most likely between freshwater and marine aquatic environments.

CONCLUSIONS

This study indicates the need for knowledge of system-specific considerations when stable isotopes are applied to ascribe Hg sources. Specifically, the results indicate that sunlight-induced changes in Hg isotope values ($\Delta^{199}Hg$ and $\delta^{202}Hg$) are highly influenced by DOM composition and concentration in the presence of plankton cells. In addition, it must also be acknowledged that in conditions with phytoplankton, $\delta^{202}Hg$ may also be subject to fractionation by other transformation processes including, but not limited to, microbial reduction,[52] uptake,[30] and sorption.[54] Our findings have implications in the field of Hg stable isotopes, specifically, the comparison of $\Delta^{199}Hg$ across diverse aquatic sites and the application of photochemical corrections of $\delta^{202}Hg$. Photochemical degradation patterns observed across a wide range of DOM types demonstrate that the controls on phytoplankton uptake vary dramatically across environmental conditions and have not been fully assessed in mechanistic studies. The lack of experiments characterizing natural DOM samples as well as DOM-phytoplankton relationships is a current science gap and limits the extension of Hg stable isotopes to modeling efforts[83] and restricts the capability of source tracking Hg from waters to fish across large geographic regions. This work provides a basis for future characterization of planktonic MeHg uptake, photochemical degradation, and Hg isotope fractionation pathways under environmentally relevant MeHg-DOM ratios to permit the confident interpretation of Hg stable isotopes in aquatic systems.

ASSOCIATED CONTENT

Supporting Information

The Supporting Information is available free of charge at https://pubs.acs.org/doi/10.1021/acsearthspacechem.3c00154.

Additional uptake and sunlight exposure experimental methods, DOM characterization, uptake and sunlight exposure experimental concentration and isotope data summaries, and light intensity profiles during experimental irradiation period of the sunlight exposure experiment; stable isotope plots in sunlight exposure experiment; application of photochemical slopes from sunlight exposure experiment (PDF)

AUTHOR INFORMATION

Corresponding Author

Sarah E. Janssen − *U.S. Geological Survey Upper Midwest Water Science Center, Madison, Wisconsin 53726, United States;* orcid.org/0000-0003-4432-3154; Email: sjanssen@usgs.gov

Authors

Grace J. Armstrong − *U.S. Geological Survey Upper Midwest Water Science Center, Madison, Wisconsin 53726, United States; Environmental Chemistry and Technology Program,*

University of Wisconsin-Madison, Madison, Wisconsin 53706, United States

Brett A. Poulin − *Department of Environmental Toxicology, University of California Davis, Davis, California 95616, United States;* orcid.org/0000-0002-5555-7733

Michael T. Tate − *U.S. Geological Survey Upper Midwest Water Science Center, Madison, Wisconsin 53726, United States*

David P. Krabbenhoft − *U.S. Geological Survey Upper Midwest Water Science Center, Madison, Wisconsin 53726, United States;* orcid.org/0000-0003-1964-5020

James P. Hurley − *Environmental Chemistry and Technology Program, University of Wisconsin-Madison, Madison, Wisconsin 53706, United States; University of Wisconsin Aquatic Sciences Center, Madison, Wisconsin 53706, United States;* orcid.org/0000-0003-4430-5319

Complete contact information is available at: https://pubs.acs.org/10.1021/acsearthspacechem.3c00154

Notes

The authors declare no competing financial interest.

■ ACKNOWLEDGMENTS

This work was supported by the U.S. Geological Survey's National Institutes for Water Resources National Competitive 104G Grants Program (Project Number G19AP00003), the U.S. Geological Survey Toxic Substances Hydrology and Contaminants Biology Program, and the National Science Foundation (EAR-1629698). The authors thank Jocelyn C. Hemming, Dawn Perkins, Patrick Gorski, and the Ecotoxicology Team at the Wisconsin State Laboratory of Hygiene for help culturing phytoplankton stocks, and the U.S. Geological Survey Mercury Research Laboratory for assistance in mercury measurements. This research used resources of the Advanced Photon Source, a U.S. Department of Energy (DOE) Office of Science User Facility operated for the DOE Office of Science by Argonne National Laboratory under Contract No. DEAC02-06CH11357. Any use of trade, firm, or product names is for descriptive purposes only and does not imply the endorsement of the U.S. Government.

■ REFERENCES

(1) Mergler, D.; Anderson, H. A.; Chan, L. H. M.; Mahaffey, K. R.; Murray, M.; Sakamoto, M.; Stern, A. H. Methylmercury Exposure and Health Effects in Humans: A Worldwide Concern. *AMBIO: J. Human Environ.* **2007**, *36* (1), 3−11.

(2) World Health, O.. Mercury and Health 2017 https://www.who.int/news-room/fact-sheets/detail/mercury-and-health.

(3) UN Environment Programme, C. a.. *Health Branch Geneva, S, Global Mercury Assessment 2018*, UN Environment Programme2019.

(4) Hammerschmidt, C. R.; Finiguerra, M. B.; Weller, R. L.; Fitzgerald, W. F. Methylmercury Accumulation in Plankton on the Continental Margin of the Northwest Atlantic Ocean. *Environ. Sci. Technol.* **2013**, *47* (8), 3671−3677.

(5) Pickhardt, P. C.; Fisher, N. S. Accumulation of Inorganic and Methylmercury by Freshwater Phytoplankton in Two Contrasting Water Bodies. *Environ. Sci. Technol.* **2007**, *41* (1), 125−131.

(6) Seller, P.; Kelly, C. A.; Rudd, J. W. M.; MacHutchon, A. R. Photodegradation of Methylmercury in Lakes. *Nature* **1996**, *380* (6576), 694−697.

(7) Krabbenhoft, D. P.; Olson, M. L.; Dewild, J. F.; Clow, D. W.; Striegl, R. G.; Dornblaser, M. M.; Vanmetre, P. Mercury Loading and Methylmercury Production and Cycling in High-Altitude Lakes from the Western United States. *Water, Air, Soil Pollut.: Focus* **2002**, *2*, 233−249.

(8) Hammerschmidt, C. R.; Fitzgerald, W. F.; Lamborg, C. H.; Balcom, P. H.; Tseng, C. M. Biogeochemical Cycling of Methylmercury in Lakes and Tundra Watersheds of Arctic Alaska. *Environ. Sci. Technol.* **2006**, *40* (4), 1204−1211.

(9) Black, F. J.; Poulin, B. A.; Flegal, A. R. Factors Controlling the Abiotic Photo-degradation of Monomethylmercury in Surface Waters. *Geochim. Cosmochim. Acta* **2012**, *84*, 492−507.

(10) Schaefer, J. K.; Yagi, J.; Reinfelder, J. R.; Cardona, T.; Ellickson, K. M.; Tel-Or, S.; Barkay, T. Role of the Bacterial Organomercury Lyase (*MerB*) in Controlling Methylmercury Accumulation in Mercury-contaminated Natural Waters. *Environ. Sci. Technol.* **2004**, *38* (16), 4304−4311.

(11) Ravichandran, M. Interactions Between Mercury and Dissolved Organic Matter−−A Review. *Chemosphere* **2004**, *55* (3), 319−331.

(12) Skrobonja, A.; Gojkovic, Z.; Soerensen, A. L.; Westlund, P.-O.; Funk, C.; Björn, E. Uptake Kinetics of Methylmercury in a Freshwater Alga Exposed to Methylmercury Complexes with Environmentally Relevant Thiols. *Environ. Sci. Technol.* **2019**, *53* (23), 13757−13766.

(13) Amirbahman, A.; Reid, A. L.; Haines, T. A.; Kahl, J. S.; Arnold, C. Association of Methylmercury with Dissolved Humic Acids. *Environ. Sci. Technol.* **2002**, *36* (4), 690−695.

(14) Qian, Y.; Yin, X.; Lin, H.; Rao, B.; Brooks, S. C.; Liang, L.; Gu, B. Why Dissolved Organic Matter Enhances Photodegradation of Methylmercury. *Environ. Sci. Technol. Lett.* **2014**, *1* (10), 426−431.

(15) Zhang, X.; Li, Y.; Feng, G.; Tai, C.; Yin, Y.; Cai, Y.; Liu, J. Probing the DOM-mediated Photodegradation of Methylmercury by Using Organic Ligands with Different Molecular Structures as the DOM Model. *Water Res.* **2018**, *138*, 264−271.

(16) Villacorte, L. O.; Ekowati, Y.; Neu, T. R.; Kleijn, J. M.; Winters, H.; Amy, G.; Schippers, J. C.; Kennedy, M. D. Characterisation of Algal Organic Matter Produced by Bloom-forming Marine and Freshwater Algae. *Water Res.* **2015**, *73*, 216−230.

(17) Lee, C.-S.; Fisher, N. S. Methylmercury Uptake by Diverse Marine Phytoplankton. *Limnol. Oceanogr.* **2016**, *61* (5), 1626−1639.

(18) Moye, H. A.; Miles, C. J.; Phlips, E. J.; Sargent, B.; Merritt, K. K. Kinetics and Uptake Mechanisms for Monomethylmercury between Freshwater Algae and Water. *Environ. Sci. Technol.* **2002**, *36* (16), 3550−3555.

(19) Gorski, P. R.; Armstrong, D. E.; Hurley, J. P.; Shafer, M. M. Speciation of Aqueous Methylmercury Influences Uptake by a Freshwater Alga (*Selenastrum capricornutum*). *Environ. Toxicol. Chem.* **2006**, *25* (2), 534−540.

(20) Gorski, P. R.; Armstrong, D. E.; Hurley, J. P.; Krabbenhoft, D. P. Influence of Natural Dissolved Organic Carbon on the Bioavailability of Mercury to a Freshwater Alga. *Environ. Pollut.* **2008**, *154* (1), 116−123.

(21) Zhong, H.; Wang, W.-X. Controls of Dissolved Organic Matter and Chloride on Mercury Uptake by a Marine Diatom. *Environ. Sci. Technol.* **2009**, *43* (23), 8998−9003.

(22) Luengen, A. C.; Fisher, N. S.; Bergamaschi, B. A. Dissolved Organic Matter Reduces Algal Accumulation of Methylmercury. *Environ. Toxicol. Chem.* **2012**, *31* (8), 1712−1719.

(23) Seelen, E.; Liem-Nguyen, V.; Wunsch, U.; Baumann, Z.; Mason, R.; Skyllberg, U.; Bjorn, E. Dissolved Organic Matter Thiol Concentrations Determine Methylmercury Bioavailability Across the Terrestrial-marine Aquatic Continuum. *Nat. Commun.* **2023**, *14* (1), No. 6728.

(24) Bergquist, B. A.; Blum, J. D. Mass-Dependent and -Independent Fractionation of Hg Isotopes by Photoreduction in Aquatic Systems. *Science* **2007**, *318* (5849), 417−420.

(25) Chandan, P.; Ghosh, S.; Bergquist, B. A. Mercury Isotope Fractionation during Aqueous Photoreduction of Monomethylmercury in the Presence of Dissolved Organic Matter. *Environ. Sci. Technol.* **2015**, *49* (1), 259−267.

(26) Rose, C. H.; Ghosh, S.; Blum, J. D.; Bergquist, B. A. Effects of Ultraviolet Radiation on Mercury Isotope Fractionation during

Photo-reduction for Inorganic and Organic Mercury Species. *Chem. Geol.* **2015**, *405*, 102−111.
(27) Bouchet, S.; Tessier, E.; Masbou, J.; Point, D.; Lazzaro, X.; Monperrus, M.; Guédron, S.; Acha, D.; Amouroux, D. In Situ Photochemical Transformation of Hg Species and Associated Isotopic Fractionation in the Water Column of High-Altitude Lakes from the Bolivian Altiplano. *Environ. Sci. Technol.* **2022**, *56* (4), 2258−2268.
(28) Kritee, K.; Motta, L. C.; Blum, J. D.; Tsui, M. T. K.; Reinfelder, J. R. Photomicrobial Visible Light-Induced Magnetic Mass Independent Fractionation of Mercury in a Marine Microalga. *ACS Earth Space Chem.* **2018**, *2* (5), 432−440.
(29) Zheng, W.; Hintelmann, H. Isotope Fractionation of Mercury during Its Photochemical Reduction by Low-Molecular-Weight Organic Compounds. *J. Phys. Chem. A* **2010**, *114* (12), 4246−4253.
(30) Wang, Y.; Janssen, S. E.; Schaefer, J. K.; Yee, N.; Reinfelder, J. R. Tracing the Uptake of Hg(II) in an Iron-Reducing Bacterium Using Mercury Stable Isotopes. *Environ. Sci. Technol. Lett.* **2020**, *7* (8), 573−578.
(31) Janssen, S. E.; Schaefer, J. K.; Barkay, T.; Reinfelder, J. R. Fractionation of Mercury Stable Isotopes during Microbial Methylmercury Production by Iron- and Sulfate-Reducing Bacteria. *Environ. Sci. Technol.* **2016**, *50* (15), 8077−8083.
(32) Agency, U. S. E. P.. *Short-term Methods for Estimating the Chronic Toxicity of Effluents and Receiving Waters to Freshwater Organisms*, 2002350.
(33) Brown, R. M.; Larson, D. A.; Bold, H. C. Airborne Algae: Their Abundance and Heterogeneity. *Science* **1964**, *143* (3606), 583−585.
(34) Nichols, H. W.; Bold, H. C. *Trichosarcina polymorpha* Gen. et Sp. Nov. *J. Phycol.* **1965**, *1* (1), 34−38.
(35) LB (Luria-Bertani) Liquid Medium *Cold Spring Harbor Protocols* 2006; Vol. *2006*1 DOI: 10.1101/pdb.rec8141.
(36) Morel, F. M. M.; Westall, J. C.; Reuter, J. G.; Chaplick, J. P. *Description of the Algal Growth Media 'Aquil'and 'Fraquil'. Water Quality Laboratory, Ralph Parsons Laboratory for Water Resources and Hydrodynamics*; Massachusetts Institute of Technology, 1975.
(37) Price, N. M.; Harrison, G. I.; Hering, J. G.; Hudson, R. J.; Nirel, P. M. V.; Palenik, B.; Morel, F. M. M. Preparation and Chemistry of the Artificial Algal Culture Medium Aquil. *Biol. Oceanogr.* **1989**, *6* (5−6), 443−461.
(38) International Humic Substances Society. humic-substances.org, 2022.
(39) Gerbig, C. A.; Kim, C. S.; Stegemeier, J. P.; Ryan, J. N.; Aiken, G. R. Formation of Nanocolloidal Metacinnabar in Mercury-DOM-Sulfide Systems. *Environ. Sci. Technol.* **2011**, *45* (21), 9180−9187.
(40) Cao, X.; Aiken, G. R.; Butler, K. D.; Mao, J.; Schmidt-Rohr, K. Comparison of the Chemical Composition of Dissolved Organic Matter in Three Lakes in Minnesota. *Environ. Sci. Technol.* **2018**, *52* (4), 1747−1755.
(41) Poulin, B. A.; Ryan, J. N.; Nagy, K. L.; Stubbins, A.; Dittmar, T.; Orem, W.; Krabbenhoft, D. P.; Aiken, G. R. Spatial Dependence of Reduced Sulfur in Everglades Dissolved Organic Matter Controlled by Sulfate Enrichment. *Environ. Sci. Technol.* **2017**, *51* (7), 3630−3639.
(42) Manceau, A.; Nagy, K. L. Quantitative Analysis of Sulfur Functional Groups in Natural Organic Matter by XANES Spectroscopy. *Geochim. Cosmochim. Acta* **2012**, *99*, 206−223.
(43) Haitzer, M.; Aiken, G. R.; Ryan, J. N. Binding of Mercury (II) to Aquatic Humic Substances: Influence of pH and Source of Humic Substances. *Environ. Sci. Technol.* **2003**, *37* (11), 2436−2441.
(44) Armstrong, G. J.; Janssen, S. E.; Tate, M. T. Measurements of Mercury Stable Isotopes during Photochemical Demethylation of Methylmercury: U.S. Geological Survey data release, 2023.
(45) Potter, B. B.; Wimsatt, J. C. *Method 415.3. Measurement of Total Organic Carbon, Dissolved Organic Carbon and Specific UV Absorbance at 254 nm in Source Water and Drinking Water*; US Environmental protection agency: Washington, DC, 2005.
(46) Poulin, B. A. Selective Photochemical Oxidation of Reduced Dissolved Organic Sulfur to Inorganic Sulfate. *Environ. Sci. Technol. Lett.* **2023**, *10*, 499−505.
(47) Li, Z.; Wu, Z.; Shao, B.; Tanentzap, A. J.; Chi, J.; He, W.; Liu, Y.; Wang, X.; Zhao, Y.; Tong, Y. Biodegradability of Algal-derived Dissolved Organic Matter and its Influence on Methylmercury Uptake by Phytoplankton. *Water Res.* **2023**, *242*, No. 120175.
(48) Janssen, S. E.; Lepak, R. F.; Tate, M. T.; Ogorek, J. M.; DeWild, J. F.; Babiarz, C. L.; Hurley, J. P.; Krabbenhoft, D. P. Rapid Preconcentration of Mercury in Solids and Water for Isotopic Analysis. *Anal. Chim. Acta* **2019**, *1054*, 95−103.
(49) Yin, R.; Krabbenhoft, D. P.; Bergquist, B. A.; Zheng, W.; Lepak, R. F.; Hurley, J. P. Effects of Mercury and Thallium Concentrations on High Precision Determination of Mercury Isotopic Composition by Neptune Plus Multiple Collector Inductively Coupled Plasma Mass Spectrometry. *J. Anal. At. Spectrom.* **2016**, *31* (10), 2060−2068.
(50) Blum, J. D.; Bergquist, B. A. Reporting of Variations in the Natural Isotopic Composition of Mercury. *Anal. Bioanal. Chem.* **2007**, *388* (2), 353−359.
(51) National Institute of Standards & Technology. Report of Investigation, RM 8610 - Mercury Isotopes in UM-Almaden Mono-Elemental Secondary Standard *Standard Reference Materials*.
(52) Grégoire, D. S.; Janssen, S. E.; Lavoie, N. C.; Tate, M. T.; Poulain, A. J. Stable Isotope Fractionation Reveals Similar Atomic-Level Controls during Aerobic and Anaerobic Microbial Hg Transformation Pathways. *Appl. Environ. Microbiol.* **2021**, *87* (18), No. e00678-21.
(53) Ogorek, J. M.; Lepak, R. F.; Hoffman, J. C.; DeWild, J. F.; Rosera, T. J.; Tate, M. T.; Hurley, J. P.; Krabbenhoft, D. P. Enhanced Susceptibility of Methylmercury Bioaccumulation into Seston of the Laurentian Great Lakes. *Environ. Sci. Technol.* **2021**, *55* (18), 12714−12723.
(54) Jiskra, M.; Wiederhold, J. G.; Bourdon, B.; Kretzschmar, R. Solution Speciation Controls Mercury Isotope Fractionation of Hg (II) Sorption to Goethite. *Environ. Sci. Technol.* **2012**, *46* (12), 6654−6662.
(55) Barkay, T.; Wagner-Döbler, I. Microbial Transformations of Mercury: Potentials, Challenges, and Achievements in Controlling Mercury Toxicity in the Environment. In *Advances in Applied Microbiology*; Academic Press, 2005; Vol. *57*, pp 1−52.
(56) Grégoire, D. S.; Poulain, A. J. A Little Bit of Light Goes a Long Way: The Role of Phototrophs on Mercury Cycling. *Metallomics* **2014**, *6* (3), 396−407.
(57) Lanzillotta, E.; Ceccarini, C.; Ferrara, R.; Dini, F.; Frontini, F. P.; Banchetti, R. Importance of the Biogenic Organic Matter in Photoformation of Dissolved Gaseous Mercury in a Culture of the Marine Diatom *Chaetoceros* sp. *Sci. Total Environ.* **2004**, *318* (1−3), 211−221.
(58) Boyd, E. S.; Barkay, T. The Mercury Resistance Operon: From an Origin in a Geothermal Environment to an Efficient Detoxification Machine. *Front. Microbiol.* **2012**, *3*, No. 349.
(59) Kritee, K.; Barkay, T.; Blum, J. D. Mass Dependent Stable Isotope Fractionation of Mercury during *mer* Mediated Microbial Degradation of Monomethylmercury. *Geochim. Cosmochim. Acta* **2009**, *73* (5), 1285−1296.
(60) Tsui, M. T.-K.; Blum, J. D.; Kwon, S. Y. Review of Stable Mercury Isotopes in Ecology and Biogeochemistry. *Sci. Total Environ.* **2020**, *716*, No. 135386.
(61) Blum, J. D.; Sherman, L. S.; Johnson, M. W. Mercury Isotopes in Earth and Environmental Sciences. *Annu. Rev. Earth Planet. Sci.* **2014**, *42*, 249−269.
(62) Zheng, W.; Hintelmann, H. Mercury Isotope Fractionation During Photoreduction in Natural Water is Controlled by its Hg/DOC Ratio. *Geochim. Cosmochim. Acta* **2009**, *73* (22), 6704−6715.
(63) Zheng, W.; Demers, J. D.; Lu, X.; Bergquist, B. A.; Anbar, A. D.; Blum, J. D.; Gu, B. Mercury Stable Isotope Fractionation during Abiotic Dark Oxidation in the Presence of Thiols and Natural Organic Matter. *Environ. Sci. Technol.* **2019**, *53* (4), 1853−1862.
(64) Kritee, K.; Blum, J. D.; Reinfelder, J. R.; Barkay, T. Microbial Stable Isotope Fractionation of Mercury: A Synthesis of Present Understanding and Future Directions. *Chem. Geol.* **2013**, *336*, 13−25.
(65) Motta, L. C.; Kritee, K.; Blum, J. D.; Tsui, M. T.-K.; Reinfelder, J. R. Mercury Isotope Fractionation during the Photochemical

Reduction of Hg(II) Coordinated with Organic Ligands. *J. Phys. Chem. A* **2020**, *124* (14), 2842−2853.
(66) Romera-Castillo, C.; Jaffé, R. Free Radical Scavenging (Antioxidant Activity) of Natural Dissolved Organic Matter. *Mar. Chem.* **2015**, *177*, 668−676.
(67) Grégoire, D. S.; Poulain, A. J. Shining Light on Recent Advances in Microbial Mercury Cycling. *Facets* **2018**, *3*, 858−879, DOI: 10.1139/facets-2018-0015.
(68) Kritee, K.; Blum, J. D.; Johnson, M. W.; Bergquist, B. A.; Barkay, T. Mercury Stable Isotope Fractionation during Reduction of Hg (II) to Hg (0) by Mercury Resistant Microorganisms. *Environ. Sci. Technol.* **2007**, *41* (6), 1889−1895.
(69) Lepak, R. F.; Janssen, S. E.; Yin, R.; Krabbenhoft, D. P.; Ogorek, J. M.; Dewild, J. F.; Tate, M. T.; Holsen, T. M.; Hurley, J. P. Factors Affecting Mercury Stable Isotopic Distribution in Piscivorous Fish of the Laurentian Great Lakes. *Environ. Sci. Technol.* **2018**, *52* (5), 2768−2776.
(70) Blum, J. D.; Popp, B. N.; Drazen, J. C.; Choy, C. A.; Johnson, M. W. Methylmercury Production Below the Mixed Layer in the North Pacific Ocean. *Nat. Geosci.* **2013**, *6* (10), 879−884.
(71) Janssen, S. E.; Riva-Murray, K.; DeWild, J. F.; Ogorek, J. M.; Tate, M. T.; Van Metre, P. C.; Krabbenhoft, D. P.; Coles, J. F. Chemical and Physical Controls on Mercury Source Signatures in Stream Fish from the Northeastern United States. *Environ. Sci. Technol.* **2019**, *53* (17), 10110−10119.
(72) Senn, D. B.; Chesney, E. J.; Blum, J. D.; Bank, M. S.; Maage, A.; Shine, J. P. Stable Isotope (N, C, Hg) Study of Methylmercury Sources and Trophic Transfer in the Northern Gulf of Mexico. *Environ. Sci. Technol.* **2010**, *44* (5), 1630−1637.
(73) Cransveld, A.; Amouroux, D.; Tessier, E.; Koutrakis, E.; Ozturk, A. A.; Bettoso, N.; Mieiro, C. L.; Berail, S.; Barre, J. P. G.; Sturaro, N.; et al. Mercury Stable Isotopes Discriminate Different Populations of European Seabass and Trace Potential Hg Sources Around Europe. *Environ. Sci. Technol.* **2017**, *51* (21), 12219−12228.
(74) Madigan, D. J.; Li, M.; Yin, R.; Baumann, H.; Snodgrass, O. E.; Dewar, H.; Krabbenhoft, D. P.; Baumann, Z.; Fisher, N. S.; Balcom, P.; Sunderland, E. M. Mercury Stable Isotopes Reveal Influence of Foraging Depth on Mercury Concentrations and Growth in Pacific Bluefin Tuna. *Environ. Sci. Technol.* **2018**, *52* (11), 6256−6264.
(75) Motta, L. C.; Blum, J. D.; Johnson, M. W.; Umhau, B. P.; Popp, B. N.; Washburn, S. J.; Drazen, J. C.; Benitez-Nelson, C. R.; Hannides, C. C. S.; Close, H. G.; Lamborg, C. H. Mercury Cycling in the North Pacific Subtropical Gyre as Revealed by Mercury Stable Isotope Ratios. *Global Biogeochem. Cycles* **2019**, *33* (6), 777−794.
(76) Kwon, S. Y.; Blum, J. D.; Chen, C. Y.; Meattey, D. E.; Mason, R. P. Mercury Isotope Study of Sources and Exposure Pathways of Methylmercury in Estuarine Food Webs in the Northeastern US. *Environ. Sci. Technol.* **2014**, *48* (17), 10089−10097.
(77) Gehrke, G. E.; Blum, J. D.; Slotton, D. G.; Greenfield, B. K. Mercury Isotopes Link Mercury in San Francisco Bay Forage Fish to Surface Sediments. *Environ. Sci. Technol.* **2011**, *45* (4), 1264−1270.
(78) Rosera, T. J.; Janssen, S. E.; Tate, M. T.; Lepak, R. F.; Ogorek, J. M.; DeWild, J. F.; Krabbenhoft, D. P.; Hurley, J. P. Methylmercury Stable Isotopes: New Insights on Assessing Aquatic Food Web Bioaccumulation in Legacy Impacted Regions. *ACS ES&T Water* **2022**, *2*, 701−709.
(79) Janssen, S. E.; Johnson, M. W.; Blum, J. D.; Barkay, T.; Reinfelder, J. R. Separation of Monomethylmercury from Estuarine Sediments for Mercury Isotope Analysis. *Chem. Geol.* **2015**, *411*, 19−25.
(80) Qin, C.; Chen, M.; Yan, H.; Shang, L.; Yao, H.; Li, P.; Feng, X. Compound Specific Stable Isotope Determination of Methylmercury in Contaminated Soil. *Sci. Total Environ.* **2018**, *644*, 406−412.
(81) Tsui, M. T. K.; Blum, J. D.; Kwon, S. Y.; Finlay, J. C.; Balogh, S. J.; Nollet, Y. H. Sources and Transfers of Methylmercury in Adjacent River and Forest Food Webs. *Environ. Sci. Technol.* **2012**, *46* (20), 10957−10964.
(82) Tsui, M.-K.; Blum, J. D.; Finlay, J. C.; Balogh, S. J.; Nollet, Y. H.; Palen, W. J.; Power, M. E. Variation in Terrestrial and Aquatic Sources of Methylmercury in Stream Predators as Revealed by Stable Mercury Isotopes. *Environ. Sci. Technol.* **2014**, *48* (17), 10128−10135.
(83) Sun, R.; Jiskra, M.; Amos, H. M.; Zhang, Y.; Sunderland, E. M.; Sonke, J. E. Modelling the Mercury Stable Isotope Distribution of Earth Surface Reservoirs: Implications for Global Hg Cycling. *Geochim. Cosmochim. Acta* **2019**, *246*, 156−173.